Target journal: Neurology: Neuroimmunology & Neuroinflammation

Different fumaric acid esters elicit distinct pharmacological responses

Brian T. Wipke, PhD*§, Robert Hoepner, MD*, Katrin Strassburger-Krogias, MD, Ankur M. Thomas, MS, Davide Gianni, PhD, Suzanne Szak, PhD, Melanie S. Brennan, PhD§, Maximilian Pistor, MD, Ralf Gold, MD, PhD, Andrew Chan, MD†, and Robert H. Scannevin, PhD†§

*These authors contributed equally to the manuscript.

†These authors contributed equally to the manuscript.

§employee of Biogen at the time the research was conducted

Brian T. Wipke, Biogen, Inc., Cambridge, MA; Robert Hoepner, Department of Neurology, Inselspital, Bern University Hospital, University of Bern, Bern, Switzerland; Katrin Strassburger-Krogias, Department of Neurology, St. Josef Hospital, Ruhr University Bochum, Bochum, Germany; Ankur M. Thomas, Biogen, Inc., Cambridge, MA; Davide Gianni, Biogen, Inc., Cambridge, MA; Suzanne Szak, Biogen, Inc., Cambridge, MA; Melanie S. Brennan, Biogen, Inc., Cambridge, MA; Maximilian Pistor, Department of Neurology, Inselspital, Bern University Hospital, University of Bern, Bern, Switzerland; Ralf Gold, Department of Neurology, St. Josef Hospital, Ruhr University Bochum, Bochum, Germany; Andrew Chan, Department of Neurology, Inselspital, Bern University Hospital,

University of Bern, Bern, Switzerland; Robert H. Scannevin, Biogen, Inc., Cambridge, MA.

Supplemental Data

Figures: figure e-1.

Tables: table e-1 and table e-2.

Correspondence

Dr. Andrew Chan
Department of Neurology, Inselspital, Bern University Hospital, University of Bern, Bern, Switzerland
Telephone number: +41 31 632 76 95
Email: Andrew.Chan@insel.ch

Suzanne Szak
Biogen, Inc., Cambridge, MA, USA
Telephone number: +1-617-679-4923
Email: suzanne.szak@biogen.com

Word counts

Manuscript: (≤3500 for manuscript) 3471 words

Abstract: (≤250 for abstract) 272 words

Introduction: (≤250) 243 words

47 **References:** 27

48 **Tables and figures:** 5 (1 table, 4 figures)

49

50 **Study funding:** Study supported by Biogen

51 **Search terms (max 5):** Multiple sclerosis [41], All Demyelinating disease (CNS)

52 [40]

53

Disclosure

This study was sponsored by Biogen.

B. T. Wipke, M. S. Brennan, and R. H. Scannevin were employees of and held stock/stock options in Biogen at the time this research was conducted. R. Hoepner received funding and personal compensation for speaker honoraria from Almirall, Biogen, Celgene, Merck, Novartis, Roche, and Sanofi. A. Thomas, D. Gianni, and S. Szak are employees of and hold stock/stock options in Biogen. K. Strassburger-Krogias received travel grants from Biogen and Merck Serono. M. Pistor reports no disclosures. R. Gold received honoraria/research support from Bayer, Biogen, Merck Serono, Novartis, and Teva, and compensation from Sage for serving as editor of *Therapeutic Advances in Neurological Disorders*. A. Chan received compensation for advisory or speaker activities for Actelion, Almirall, Bayer, Biogen, Celgene, Merck, Novartis, Roche, Sanofi, and Teva, all for hospital research funds, received research support from Biogen, Sanofi, and UCB, and receives compensation from Wiley for serving as associate editor of *European Journal of Neurology*, all for hospital research funds.

Acknowledgments

Preclinical species work was supported by Biogen, Inc. (Cambridge, MA). Karyn M. Myers, PhD, of Biogen provided initial editing support based on input from authors. Biogen also provided funding to Excel Scientific Solutions for medical writing support in the development of this paper; Karen Spach, PhD from Excel Scientific Solutions incorporated author comments, and Miranda Dixon from

Excel Scientific Solutions copyedited and styled the manuscript per journal requirements. The authors had full editorial control of the paper, and provided their final approval of all content. We thank Raghavendra Hosur, Kristopher W. King, Norm Allaire, Patrick Cullen, Alice Thai, Alex Chou, Theresa A. Hillery, Kejie Li, Liyu Yang, Chaoran Huang, and Norman Kim for their contributions to this study.

Abstract (297 words)

Objective

In order to test the hypothesis that dimethyl fumarate (DMF, Tecfidera®) elicits different biological changes from DMF combined with monoethyl fumarate (MEF) (Fumaderm®, a psoriasis therapy), we investigated DMF and MEF in rodents and cynomolgus monkeys. Possible translatability of findings was explored with lymphocyte counts from a retrospective cohort of MS patients.

Methods

In rodents, we evaluated pharmacokinetic and pharmacodynamic effects induced by DMF and MEF monotherapies or in combination (DMF/MEF). Clinical implications were investigated in a retrospective, observational analysis of MS patients treated with DMF/MEF (n = 36).

Results

In rodents and cynomolgus monkeys, monomethyl fumarate (MMF, the primary metabolite of DMF) exhibited a higher brain penetration, whereas MEF was preferentially partitioned into the kidney. In mice, transcriptional profiling for DMF and MEF alone identified both common and distinct pharmacodynamic responses, with almost no overlap between DMF- and MEF-induced differentially expressed gene profiles in immune tissues. The nuclear factor (erythroid-derived 2)-like 2 (Nrf2)-mediated oxidative stress response pathway was exclusively regulated by DMF, whereas MEF activated apoptosis pathways. DMF/MEF

treatment demonstrated that DMF and MEF functionally interact to modify DMF- and MEF-specific responses in unpredictable ways. In MS patients, DMF/MEF treatment led to early and pronounced lymphocyte suppression, predominantly $CD8^+$ T cells.

In a multivariate regression analysis, absolute lymphocyte count (ALC) was associated with age at therapy start, baseline ALC, and DMF/MEF dosage, but not with previous immunosuppressive medication and gender.

Further, ALC increased in a small cohort of MS patients (n = 6/7) after switching from DMF/MEF to DMF monotherapy.

Conclusions

Fumaric acid esters (FAEs) exhibit different biodistribution and may elicit different biological responses; furthermore, pharmacodynamic effects of combinations differ unpredictably from monotherapy. Strong potential to induce lymphopenia in MS patients may be a result of activation of apoptosis pathways by MEF compared with DMF.

Glossary

ALC = absolute lymphocyte count; **DEG** = differentially expressed gene; **DMF** = dimethyl fumarate; **FAE** = fumaric acid esters; **GAPDH** = glyceraldehyde 3-phosphate dehydrogenase; **GCRMA** = GC-content-based Robust Multi-Array Average; **GSH** = glutathione; **IACUC** = Institutional Animal Care and Use Committee; **ILN** = inguinal lymph node; **IPA** = Ingenuity Pathway Analysis; **IQR** =

130 interquartile range; **Keap1** = Kelch-like ECH-associated protein 1; **LI** =

131 lymphopenia index; **MEF** = monoethyl fumarate; **MLN** = mesenteric lymph node;

132 **MMF** = monomethyl fumarate; **MS** = multiple sclerosis; **Nrf2** = nuclear factor

133 (erythroid-derived 2)-like 2; **QC** = quality control; **RQS** = RNA Quality Score;

134 **RRMS** = relapsing remitting multiple sclerosis; **WBC** = white blood cell count.

Introduction (≤250, currently 235)

Multiple sclerosis (MS) is a chronic inflammatory, demyelinating, autoimmune disease of the CNS.[1] During different MS disease stages, oxidative stress precipitated by mitochondrial damage also may contribute to oligodendrocyte and neuronal injury.[2] Fumaric acid esters (FAE) exhibit pleiotropic immunomodulatory effects, as well as antioxidative properties. The FAE, dimethyl fumarate (DMF), which has monomethyl fumarate (MMF) as its primary metabolite, is an oral treatment approved for use in patients with relapsing-remitting MS (RRMS),[3, 4] clinically isolated syndrome, and active secondary progressive MS.[3] Efficacy of DMF and a combination of different salts of monoethyl fumarate (MEF) was investigated in an early exploratory study in patients with RRMS[5] and is marketed in Germany as an oral therapeutic to treat psoriasis (DMF/MEF, Fumaderm®).

It is unclear whether different FAEs are functionally equivalent and if a combination treatment could alter pharmacological properties and clinical parameters, although in vitro evidence shows that different FAEs may stimulate distinct responses.[6-8] Both DMF and MEF treatment are associated with lymphopenia in some patients; however, the underlying mechanisms and relative contributions of each FAE are unknown.[9, 10]

We hypothesized that the standard clinical regimen of DMF and DMF/MEF might have different pharmacokinetic distributions and provoke different pharmacodynamic responses. We administered FAEs (DMF, MEF, DMF/MEF) individually or at doses reflecting the Fumaderm® formulation and evaluated their

distribution in various tissues and changes in transcriptional profiles. Finally, we evaluated lymphopenia in patients with MS treated with DMF/MEF.

Materials and methods

Animals

All procedures involving animals were performed in accordance with standards established in the Guide for the Care and Use of Laboratory Animals (US National Institutes of Health). All rodent animal protocols were approved by the Biogen Institutional Animal Care and Use Committee (IACUC). Animals used included female C57BL/6 mice aged 8–10 weeks (Jackson Laboratories, Bar Harbor, ME), male Sprague Dawley rats aged 12–14 weeks (Harlan Laboratories, Indianapolis, IN or Charles River Laboratories, Wilmington, MA), or female cynomolgus monkeys weighing 2–4 kg (dosing excretion studies were conducted at Charles River Laboratories [Reno, NV] using protocols approved by their IACUC).

Compound dosing

For transcriptional profiling and biodistribution studies, C57BL/6 mice or Sprague Dawley rats were dosed with DMF, a mixture of MEF salts (Ca^{2+}, Mg^{2+}, and Zn^{2+} in the ratio 91.5%:5.2%:3.2%), or a combination of DMF and MEF salts to mimic the ratio of fumarates in Fumaderm®. DMF, MEF, and DMF/MEF were formulated as fine suspensions in 0.8% hydroxypropyl methylcellulose (vehicle) and stirred continuously throughout the studies. DMF was dosed at 100 mg/kg

(the efficacious dose in a mouse experimental autoimmune encephalomyelitis model); MEF was dosed at 79.2 mg/kg (total MEF salts) representing the proportional MEF dose in Fumaderm®; and DMF/MEF, which is reflective of the ratio of DMF:MEF salts in Fumaderm® used in the clinic, was comprised of DMF 100 mg/kg and MEF 79.2 mg/kg. Mice received either a single dose (10 mL/kg for PK) or 10 daily doses (10 mL/kg) of FAEs or vehicle-only control (0.8% hydroxypropyl methylcellulose) via oral gavage. For urine excretion studies, rats were dosed (30 mg/kg) with a mixture of DMF (55.5 %), Ca^{2+} MEF (39.8 %), Mg^{2+} MEF (2.4%), Zn^{2+} MEF (1.49%), and fumaric acid (0.98%), reflective of Fumaderm® dosing. Cynomolgus monkeys were dosed (50 mg/kg) with either DMF or a mixture of MEF salts in the same proportions used in rats and mice.

In vivo gene expression profiling

Whole blood and, after perfusion, tissues were collected from naive C57Bl/6 mice dosed with vehicle, DMF, a mixture of MEF salts, or DMF/MEF at 12 hours after the final oral dose (10-day series), and snap frozen. RNA was prepared from tissues and whole blood per standard practice. RNA integrity was assessed using the HT RNA reagent kit (part number 760410, Caliper Life Sciences, Hopkinton, MA) using a LabChip GX (PerkinElmer, Waltham, MA). RNA samples with an RNA Quality Score (RQS) >8.0 were considered high quality for microarray profiling. Sample labeling, hybridization, and scanning were performed as described[11] using an Affymetrix chip HT-MG-430 PM (Affymetrix, Santa Clara, CA). Affymetrix scans were subject to quality control (QC)

measures.[12] All sample scans that passed QC were included in the analysis; these 204 CEL files (GEO accession number GSE63343) were either pooled all together or segregated based on tissue and subjected to content-based GC-Robust Multi-Array Average (GCRMA) normalization (version 2.20.0).[13, 14]

To identify genes that change uniquely in response to DMF or MEF administration in each individual tissue, a linear modeling approach was used to fit gene expression levels (log2 transformed) according to defined groups of samples and Bayesian posterior error analysis as implemented by Smyth (Bioconductor library limma, version 3.4.5).[15] Genes were considered significantly different in DMF-vs-vehicle and MEF-vs-vehicle if they met the following criteria: (1) average normalized signal intensity >4; (2) logarithm (base 10) of odds ("lods") score >0; and (3) fold change >1.5. All calculations and analyses were carried out using R (version 2.11.1) and Bioconductor.[16]

Alternately, samples across all tissues and blood were pooled and normalized together to avoid characterizing tissue-to-tissue variability in the limited subset of tissues sampled, and to fully capture all differences in DMF/MEF responses; this approach generalized the analysis and allowed us to find those probe sets that were specifically changing due to DMF or MEF, as well as those probe sets that exhibited a DMF:MEF interaction effect. The following linear mixed model was applied to the normalized data set:

Gene Expression ~ DMF + MEF + DMF:MEF + random(tissue)

Interaction probe sets were defined as those with a Bonferroni-adjusted *p* value <0.05 for the interaction term in this model. A simpler model (without the

interaction term) was fit to probe sets that exhibited no interaction effect. Similarly, probe sets were considered significant and specific to DMF if the Bonferroni-corrected *p* value was <0.05 for the DMF term and >0.05 for the MEF term (and no interaction effect was found). MEF-specific probe sets were identified by requiring the Bonferroni-corrected *p* value to be >0.05 for DMF and <0.05 for MEF.

An in vivo MEF-DMF interaction was evaluated by analyzing the specific differentially expressed genes (DEGs) modulated when these 2 compounds were co-administered (DMF 100 mg/kg and MEF salts 79.2 mg/kg). The absolute value of the difference between (DMF – vehicle) and (combination – vehicle) was calculated for each of the identified interaction probe sets, and presented as the log2 absolute difference for each probe set. In order to identify the most highly enriched molecular pathways, the sets of DMF-specific, MEF-specific, and DMF/MEF interaction probe sets were analyzed using Ingenuity Pathway Analysis (IPA) software (Qiagen, Germantown, MD). The top 10 enriched pathways for each were compared with each other for *p* value significance.

Bioanalytical studies

For biodistribution studies, immediately following blood collection, stabilizer (sodium fluoride solution, 250 mg/mL NaF in water) was added to each blood sample (10 mg/mL final) in a chilled lithium heparin blood collection tube (to inhibit metabolism of MMF or MEF), and plasma was separated from whole blood by centrifugation. Plasma was then snap frozen on dry ice and maintained

at -80°C until analyzed. MEF and MMF were measured in all experiments. MMF represents the main metabolite of DMF, which itself cannot be detected in systemic circulation after oral administration due to rapid pre-systemic conversion in vivo. Sample extracts were evaluated by liquid chromatography tandem mass spectrometry to determine MMF and MEF levels, using absolute quantitation based on standard curves spiked in the appropriate biomatrix. Results are expressed as absolute concentration (ng/g of tissue or ng/mL of plasma) and relative concentration expressed as a percentage of plasma concentration.

To measure the renal excretion of MMF and MEF, Sprague Dawley rats received a single oral dose of 30 mg/kg DMF plus MEF salts in the Fumaderm® ratio (DMF [55.5 %], Ca^{2+} MEF [39.8 %], Mg^{2+} MEF [2.4%], Zn^{2+} MEF [1.49%], and fumaric acid [0.98%]). In a separate study, cynomolgus monkeys received a single oral dose of 50 mg/kg DMF or MEF salts. In both studies, urine was collected over a 24-hour period and analyzed for MMF and MEF levels.

Patients with MS

Patients were identified by retrospective analysis of medical records from a single university hospital. Clinical characteristics (table e-1) of the majority of patients (RRMS or relapsing progressive MS, n = 18; progressive MS, n = 17; neuromyelitis optica, n = 1) treated with DMF/MEF (Fumaderm®, mean [SD] 285 [123] mg) in this retrospective, observational, cross-sectional study were described previously.[17] Baseline values of white blood cell count (WBC) and

absolute lymphocyte count (ALC) of the DMF/MEF cohort were obtained 1 week (median and interquartile range [IQR]) before initiation of DMF/MEF and every 3 months thereafter. The 7 patients who switched from DMF/MEF to DMF switched within a mean (SD) of 0.9 (2.3) weeks (6/7 no treatment-free interval, 1 patient 6 weeks interval). In these patients, a lymphopenia index (LI) normalized for dosage of the DMF component was calculated using the following operator: (lymphocyte count during medication – baseline lymphocyte count)/mg of DMF. Statistical analyses including a multivariate regression analysis, Chi-square, and Spearman rho correlation were performed with SPSS 20 (IBM, Armonk, NY).

Standard protocol approvals, registrations, and patient consents

The retrospective observation was approved by the local ethics committee (Ruhr University Bochum; numbers 5408-15 and 4797-13) and conducted in accordance with the Declaration of Helsinki, the International Conference on Harmonisation Guideline for Good Clinical Practice, and all applicable laws and regulations.

Data availability statement

Data supporting this article can be requested via the corresponding authors.

Results

Biodistribution of DMF metabolite (MMF) and MEF in mice and rats

Thirty minutes after DMF administration by oral gavage, MMF was broadly distributed throughout the bodies of both rats and mice. MMF (dosed as DMF) achieved higher brain penetration after oral administration compared with MEF, by both absolute and relative concentration (mouse, figure 1, A vs B; rat, figure 1, C vs D). In contrast, MEF preferentially partitioned to the kidney, leading to higher absolute and relative concentration. These differences led to an increased brain to plasma ratio for DMF ($p < 0.001$) (figure 1E) and conversely higher kidney to plasma ratio for MEF compared with each other ($p < 0.01$) (figure 1F). Differences in biodistribution remained similar after a 10-day dosing period (data not shown).

Renal excretion of MMF and MEF is significantly different in rats and cynomolgus monkeys

Consistent with pharmacokinetic and tissue distribution data, mean excretion of intact MEF was significantly higher relative to MMF in rats (9-fold; $p < 0.05$) and in cynomolgus monkeys (26-fold; $p < 0.001$) (data not shown). Thus, the kidney experienced significantly greater exposure to MEF compared with MMF (after DMF dosing), which might be expected as the kidney to plasma ratio was higher for MEF.

Interaction between DMF and MEF based on gene expression changes in mice

As determined by induced gene expression changes relative to vehicle, DMF, MEF, and their combination exhibited varied pharmacodynamic activity based on tissue type, with many gene expression changes unique to either DMF or MEF exposure (figure e-1). All samples were normalized and analyzed together to identify genes that exhibit a change in expression uniquely due to DMF or MEF, as well as interaction effects between DMF and MEF. In the combined tissues data set, 487 genes were found to change specifically from DMF treatment. These genes were enriched for pathways for the nuclear factor (erythroid-derived 2)-like 2 (Nrf2)-mediated oxidative stress response, glutathione (GSH)-mediated detoxification, and other environmental sensing pathways (e.g., aryl hydrocarbon receptor signaling) (Table e-2). In total, 224 genes were identified with expression changes specifically due to MEF; they were enriched for death receptor signaling pathway, apoptosis signaling, and autophagy-related pathway. The absolute mean value of each tissue for the DMF- and MEF-specific groups was subjected to unsupervised hierarchical clustering (figure 2A). DMF specificity was more pronounced in the mesenteric lymph node (MLN), inguinal lymph node (ILN), spleen, and whole blood, whereas MEF specificity was found predominantly in the kidney and MLN. After combination therapy, 132 DEGs exhibited a significant interaction effect between DMF and MEF. The most pronounced interactions between fumarates were found in tissues related to immune function (whole blood, MLN, ILN, and spleen) (figure 2B and table e-3)

which is of interest for the relative amount of lymphocyte suppression by each fumarate compound. The unfolded protein response (a stress response) and neurodegenerative signaling (e.g., Huntington's disease, RNA polymerase III assembly, and protein degradation) pathways were uniquely enriched for DMF and MEF interaction. These biological trends were constant regardless of whether the tissues were pooled or kept separate for the analysis.

DMF/MEF combination induces fast and moderate-to-severe lymphopenia in patients with MS

To assess biological consequences in humans, effects on lymphocyte counts in patients with MS treated with DMF/MEF were retrospectively analyzed. DMF/MEF treatment led to a fast and profound reduction (44%) of ALC within the first year of treatment (figure 3 and table 2). ALCs remained suppressed beyond 12 months until the end of the observation (24 months). Using a multivariate linear regression analysis DMF/MEF dose (coef. -1.05, 95%CI -2.09 - -0.01, p=0.047), age at treatment start (coef. -13.32, 95%CI -23.61 - -3.04, p=0.01), time point of sampling (coef. -73.97, 95%CI -133.68 - -14.26, p=0.02) and baseline ALC (coef. 0.51, 95%CI 0.33 – 0.70, p<0.001) influenced ALC, whereas previous use of immunosuppressive treatments and sex did not.

Grade 2 or 3 lymphopenia was not present at baseline but occurred in 27.8% (grade 2) and 5.6% (grade 3) of patients at the second year of DMF/MEF treatment (table 1).

In 17 of 21 patients with available lymphocyte subpopulation data, the $CD4^+$:$CD8^+$ ratio correlated with ALC (Spearman rho correlation -0.52; $p = 0.02$; n = 21) and increased 1.5-fold in the first year and 2.3-fold in the second year (figure 4 and table 3). The increase in the $CD4^+$:$CD8^+$ ratio was driven by a 3.5-fold higher suppression of $CD8^+$ compared with $CD4^+$ T cells (maximum reduction of $CD4^+$ T cells 19% vs $CD8^+$ T cells 66%). Finally, we analyzed lymphocyte data longitudinally from patients who switched from DMF/MEF to DMF. In general, the LI normalized for dosage of the DMF component increased in 6 of 7 patients, with an increase of median (IQR) LI from -4.33 (4.83) to -1.04 (4.33) (Mann–Whitney U test, $p = 0.04$) after switching from DMF/MEF to DMF. In addition, when analyzing the ALC values without normalization to DMF dosage, an ALC increase in 4 of 7 patients was observed despite an increase of DMF dosage of 23%. One patient demonstrated stable ALCs, with a 100% increase in DMF dose. In the remaining 2 patients, both experienced a further decrease of ALCs, with a 78% increased DMF dose after withdrawal of MEF.

Discussion

Fumaderm® provided initial evidence of the potential therapeutic effects of fumarates in patients with MS.[17, 18] The specific in vivo pharmacokinetic, pharmacodynamic, and immunologic effects of DMF and MEF salts in Fumaderm® have not been investigated.[7] In vitro studies have demonstrated differential effects of DMF and MEF, which may provide insight to the in vivo differences observed. Specifically, differential effects of DMF and MEF were

observed for a targeted set of biological properties, including Kelch-like ECH-associated protein 1 (Keap1) modification, Nrf2 activation, and GSH consumption and biosynthesis.[7] DMF and MMF could potentially inhibit the activation of lymphoid and myeloid cells by downregulation of aerobic glycolysis via the succination and inactivation of glyceraldehyde 3-phosphate dehydrogenase (GAPDH).[19] In addition, DMF and MMF activate endogenous detoxifying and antioxidant pathway genes through binding to Keap1, activating Nrf2 transcriptional activity, and modulating GSH levels and activating GSH biosynthesis.[7, 20]

A primary goal of these studies was to determine whether coadministration of DMF and MEF would provide an additive response or trigger unique biological responses in vivo. An unbiased transcriptional approach was used to characterize the differences between DMF, MEF, and DMF/MEF under steady-state exposure in vivo. The individual contributions of DMF and MEF were explored using doses that reflected the composition of Fumaderm®. Oral administration of DMF and MEF showed significant differences in their biodistribution and excretion profiles in mice, rats, and monkeys. MEF exhibited 10- to 20-fold higher compound exposure in the kidney relative to MMF. Compared with systemic exposure, DMF levels were 4-fold higher than MEF levels in the brain. This could indicate that DMF might be more potent in directly targeting oxidative stress pathways in the CNS.

In mice, DMF showed preferential modulation of transcripts in tissues related to immune function (spleen, MLN, ILN, and whole blood), whereas MEF

showed a preference for transcript modulation in the kidney and MLN. This difference with MEF might be explained by its remarkably reduced concentration and area under the curve compared with DMF, which are likely the result of the combination of a lower relative dose and increased renal excretion. However, these effects might also be associated with individual transcriptional effects of the 2 compounds, as the number of DEGs modulated by DMF are considerably higher in organs with exposure similar to MEF, such as the kidney. It remains uncertain whether the DMF-induced transcriptional changes are mediated by MMF signaling through HCAR2[21] (expressed on myeloid cells), through Nrf2 (ubiquitously expressed in the body), or an additional pathway yet to be described. DMF likely has multiple therapeutic targets as it functions through both Nrf-2 dependent and independent pathways, indirect and/or direct inhibition of NF- κB, and modulation of oxidative stress-sensitive transcription factors and STATs through DMF-induced glutathione depletion and reactive oxygen species induction. [18, 22, 23] These analyses did not identify differential effects of DMF/MEF on Keap1 and GAPDH transcripts. In contrast, previous studies have shown post-transcriptional regulation through direct modification of activity of proteins such as Keap1 and GAPDH.[19, 24] Specifically, DMF modification of lipid metabolic pathways and impairment of aerobic glycolysis and GAPDH activity by direct modification of the GAPDH protein itself are both related to DMF-induced immunological changes.[19, 24] There are legitimate questions about whether the GAPDH preclinical data at high doses is relevant for human subjects that have much lower C_{max} levels of MMF relative to mice, but the potential exists for it to

be active in vivo. Pharmacodynamic data of DMF and MEF monotherapies andcombined DMF/MEF treatment, as well as DEG data assessing compounds' interactions, indicate that differential gene expression may be more complex than increasing potency or total dosage. It is not known whether the fumarate tissue distribution and gene-expression profiles shown in animals in this analysis differ from that in humans.

Our analyses of lymphocyte kinetics in patients with MS support the pharmacodynamic results. In patients who switched from DMF/MEF to DMF monotherapy, ALC increased even after normalization for DMF dosage. A pronounced and early reduction of ALCs during treatment with DMF/MEF was shown over a follow up of 24 months. Treatment of patients with MS with DMF/MEF led to an increase in the $CD4^+$:$CD8^+$ ratio, with a predominant reduction of $CD8^+$ cells. Similar increases in $CD4^+$:$CD8^+$ ratios were observed in DMF/MEF-treated patients with psoriasis,[9] yet this appears to be more pronounced than in patients with MS receiving DMF monotherapy (1.4-fold).[25] In a recent study, DMF monotherapy shifted the immunophenotype of circulating lymphocyte subsets, and ALC closely correlated with $CD4^+$ and $CD8^+$ T-cell counts.[26] No increased risk of serious infection was observed in patients with low T-cell subset counts.[26]

Owing to the limited sample size,-data analyses were limited, especially for T-cell subpopulations. Despite these limitations, multivariate regression analysis demonstrated that ALC was significantly forecasted by age, baseline ALC, DMF/MEF dose, as well as time point of sampling. Age and baseline ALC

are also known parameters predicting baseline ALC during DMF monotherapy, further supporting our analysis.[27] Specifically, previous analyses found that age ≥60 years and a baseline ALC <2 g/L are independent risk factors for the development of a severe lymphopenia during DMF therapy.[27] The small subpopulation of patients from our study that switched from DMF/MEF to DMF and exhibited an increase in ALC had a mean (SD) age of 54.1 (14.9) years.[28, 29] The retrospective design with intervals between testing not being well defined might introduce bias in the results.

In conclusion, our experimental and clinical data provide evidence for different immunological effector mechanisms of DMF compared with MEF. It is not clear whether these different pathways are associated with lymphopenia induced by FAEs, yet this study provides data on potential mechanisms for the individual therapies. Although several mechanisms leading to lymphopenia have been proposed (e.g., apoptosis, GSH depletion, oxidative stress, bone marrow affection), exact pathomechanisms remain elusive.[6, 7, 20, 30] Prolonged severe and moderate lymphopenia is considered a risk factor for very rare cases of progressive multifocal leukoencephalopathy in patients treated with DMF; therefore, identifying the differential effects of FAEs on lymphocyte counts is relevant for MS patient management.[26, 30]

Total 5 figures and Tables

Table 1. Distribution of lymphopenia grade 1–4 in DMF/MEF-treated patients

Lymphopenia, n/N (%)	Before DMF/MEF	1st year of DMF/MEF	2nd year of DMF/MEF	No. of patients with lymphopenia (1st and 2nd year)
No lymphopenia, >900/µl	27/28 (96.4)	24/31 (77.4)	8/18 (44.4)	21/32 (65.6)
Grade 1, 800–900/µl	1/28 (3.6)	4/31 (12.9)	4/18 (22.2)	4/32 (12.5)
Grade 2, 500–799/µl	0/28(0)	1/31 (3.2)	5/18 (27.8)	5/32 (15.6)
Grade 3, 200–500/µl	0/28 (0)	2/31 (6.5)	1/18 (5.6)	2/32 (6.3)

Abbreviations: DMF = dimethyl fumarate; MEF = monoethyl fumarate.

Table 2. White blood cell data from DMF/MEF-treated patients

Month	Mean (SEM)	N
0	1.80 (0.11)	28
3	1.49 (0.12)	18
6	1.00 (0.12)	12
9	1.14 (0.11)	14
12	1.01 (0.17)	13
15	1.10 (0.26)	10
18	1.01 (0.15)	10
21	0.98 (0.12)	4
24	1.00 (0.19)	6

The table shows absolute lymphocyte counts in DMF/MEF-treated patients. Mean (SEM) lymphocyte counts (× 10^9/L) over 3-month periods for patients treated with DMF/MEF. ALC = absolute lymphocyte count; DMF = dimethyl fumarate; MEF = monoethyl fumarate.

Table 3. $CD4^+$:$CD8^+$ ratio correlated with lymphocyte count

DMF/MEF	CD4		CD8		CD4/CD8 Ratio
	Median (IQR)	Percent change	Median (IQR)	Percent change	
Before DMF/MEF (n=5)	468 (434)		301 (194)		1.56
1st year of treatment (n=6)	374 (203)	-20%	161 (219)	-47%	2.32
2nd year of treatment (n=10)	378 (399)	-19%	103 (199)	-66%	3.69

The median and percentage change for $CD4^+$ and $CD8^+$ T cells are shown below the figure. DMF = dimethyl fumarate; IQR = interquartile range; MEF = monoethyl fumarate.

Figure 1 Tissue distribution of MEF and DMF metabolite (MMF) in mice and rats

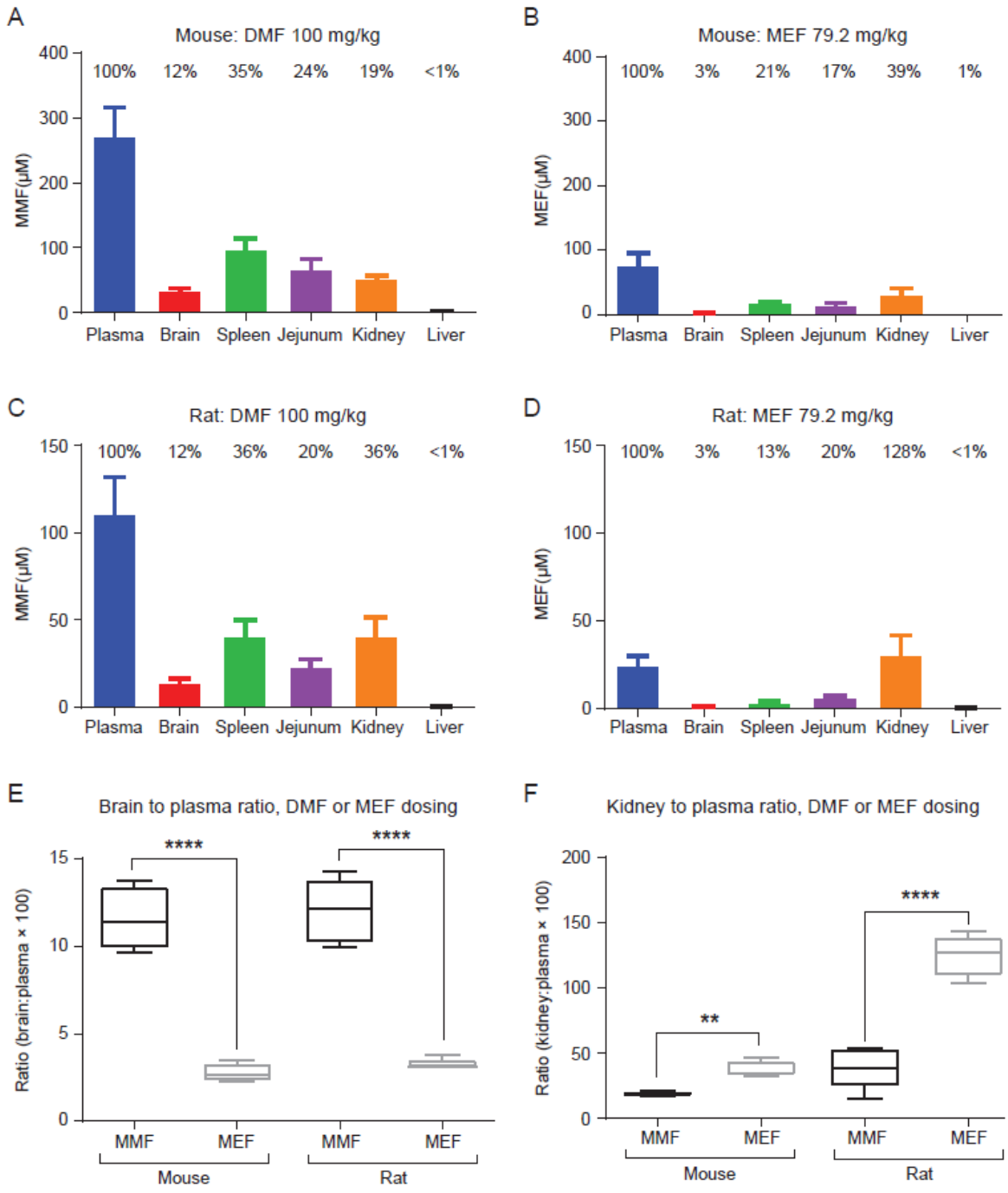

Figure 1 legend (A–D) Mice and rats were administered a single dose of DMF (100 mg/kg) (A and C) or MEF (79 mg/kg) (B and D). Plasma and tissues levels (brain, spleen, jejunum, kidney, and liver) of MEF and MMF were determined 30

minutes after dosing. Percentages above each bar represent the percent tissue penetration relative to plasma concentration. (E) Plasma to brain ratios for DMF and MEF treatment in mice and rats highlight significantly higher DMF (MMF) brain exposure ($p < 0.001$ for both species). (F) Plasma to kidney ratios for DMF and MEF treatment in mice and rats indicate significantly lower kidney exposure for DMF treatment compared with MEF ($^{**}p < 0.01$ and $^{****}p < 0.001$ in mice and rats, respectively). DMF = dimethyl fumarate; MEF = monoethyl fumarate; MMF = monomethyl fumarate.

Figure 2 (A) DMF and MEF specificity across tissues and blood and (B) magnitude of interaction effect in mice

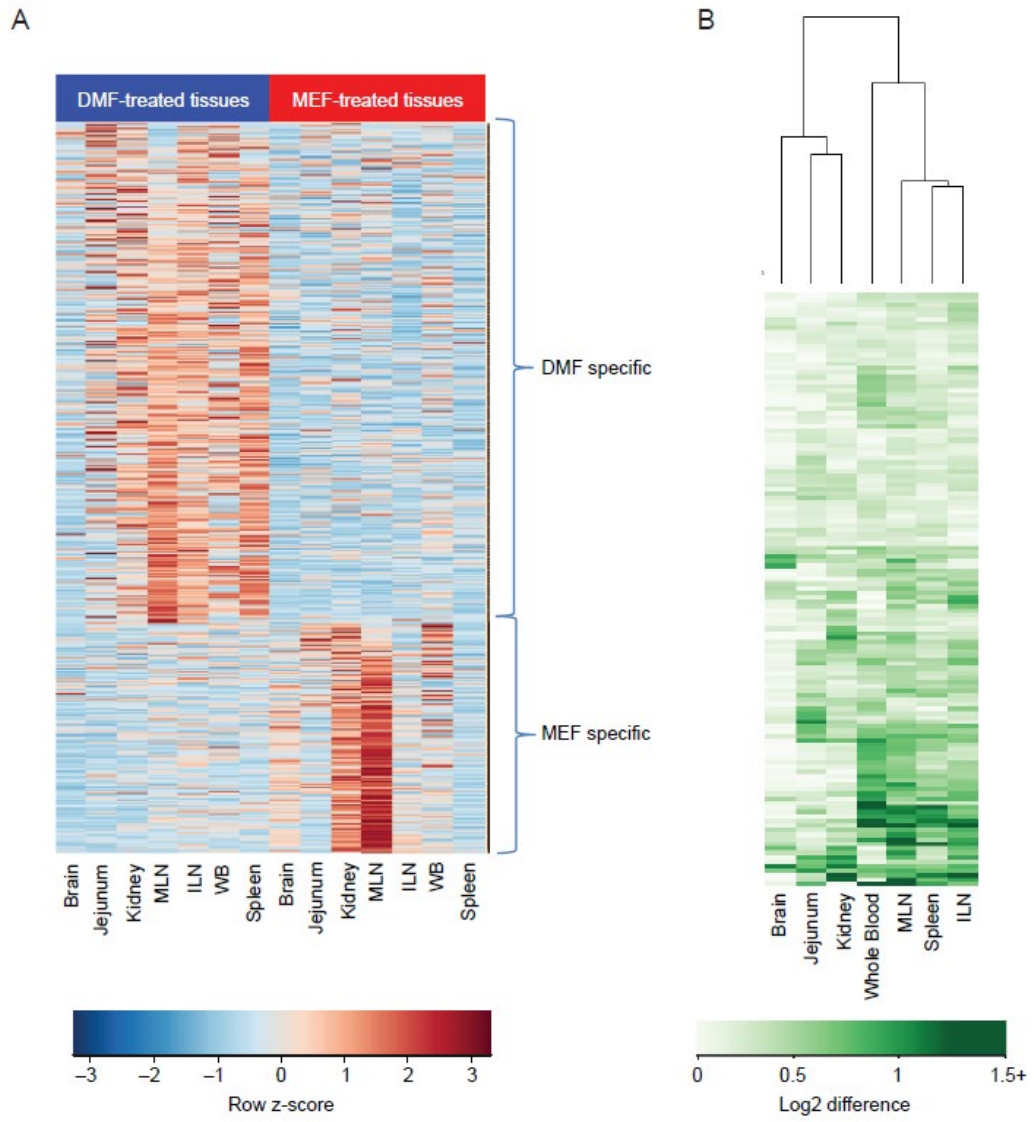

Figure 2 legend (A) After pooling all tissues, the absolute value in each tissue of the group averages (DMF – vehicle) and (MEF – vehicle) were subjected to unsupervised hierarchical clustering (n = 7 biological sample sets each) for the 487 DMF-specific and 224 MEF-specific probe sets. The relative magnitude of the degree of specificity in each tissue is shown. DMF specificity is most

pronounced in MLN, ILN, spleen, and whole blood, whereas MEF specificity is most evident in the kidney and MLN. (B) For each of the 132 interaction probe sets, the absolute value of the difference of (DMF – vehicle) and (combination – MEF) was subjected to unsupervised hierarchical clustering. The interaction effect in each tissue is shown. An interaction between DMF and MEF is most pronounced in the immunological tissues: whole blood, MLN, ILN, and spleen. DMF = dimethyl fumarate; ILN = inguinal lymph node; MEF = monoethyl fumarate; MLN = mesenteric lymph node; WBC = white blood cell.

517 **Figure 3** White blood cell data from DMF/MEF-treated patients

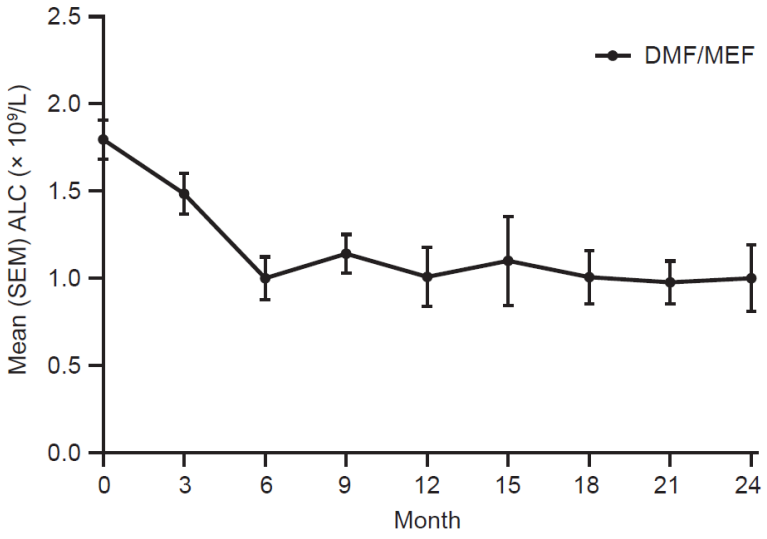

518

519

520

521 **Figure 3 legend** The figure shows absolute lymphocyte counts ł in DMF/MEF-

522 treated patients. Mean (SEM) lymphocyte counts (× 10^9/L) over 3-month periods

523 for patients treated with DMF/MEF. ALC = absolute lymphocyte count; DMF =

524 dimethyl fumarate; MEF = monoethyl fumarate.

525 **Figure 4** $CD4^+$:$CD8^+$ ratio correlated with lymphocyte count

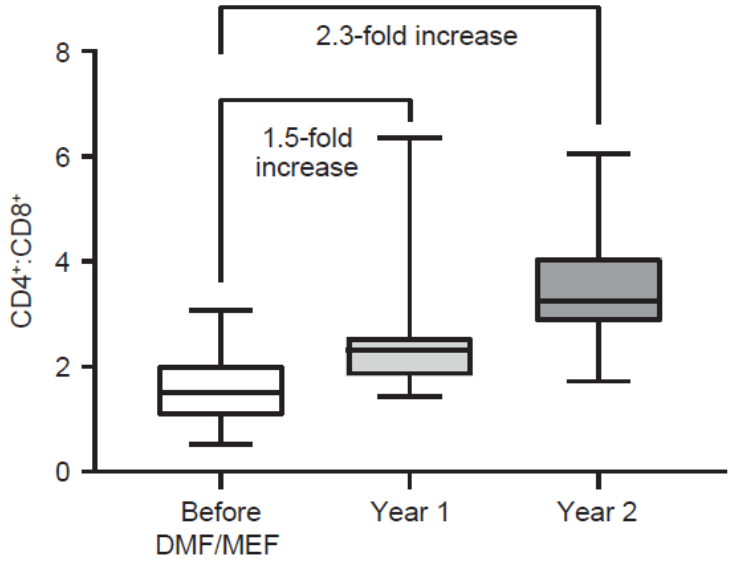

526

527 **Figure 4 legend** $CD4^+$ and $CD8^+$ T cells in patients before DMF/MEF and 1 and

528 2 years after DMF/MEF treatment. The box and whiskers plot shows median,

529 IQR, and minimum/maximum for the $CD4^+$:$CD8^+$ ratio. DMF = dimethyl fumarate;

530 IQR = interquartile range; MEF = monoethyl fumarate.

531

532 ***Supplementary tables and figures = limited to 3 figures / tables***

533 **Table e-1** Characteristics of DMF/MEF-treated patients with MS

Characteristic	Patients (N = 36)
MS disease course, n/N	
RRMS or relapsing progressive MS	18/36
Progressive MS	17/36
Neuromyelitis optica	1/36
Any previous MS medication, n/N	28/36
MS therapy within 3 months before switch, n/N	
None	26/36
Interferon-beta formulations	5/36
Fingolimod	2/36
Mitoxantrone	2/36
Azathioprine	1/36
Mean (SD) age at switch to MEF/DMF, y	56 (10.6)
Female, n/N	24/36
MS duration (SD) at switch to MEF/DMF, y	13.1 (7.8)
IV steroids at baseline (within 2 weeks), n/N	3/36
Mean (SD) IV steroids dose, mg	1167 (577)
Immunosuppressive drug in medical history, n/N	16/36
Mitoxantrone, n/N	14/36
Mean (SD) cumulative dose of mitoxantrone, mg/m^2 body surface area	73 (31.6)

Mean (SD) interval between mitoxantrone and Fumaderm©, y	2.4 (1.9)
Azathioprine, n/N	3/36
Mean (SD) interval between azathioprine and Fumaderm©, y	7.7 (6.8)
Methotrexate, n/N	2/36
Mean (SD) interval between methotrexate and Fumaderm©, y	2 (1.4)
Switch MEF/DMF to DMF	
Mean (SD) therapy durations MEF/DMF, mo	12 (8)
Mean (SD) follow-up during DMF, mo	7.7 (4.1)
No therapy-free interval, n/N	6/7
Therapy-free interval, wk (n)	6 (1)

534 Abbreviations: DMF = dimethyl fumarate; MEF = monoethyl fumarate; MS =
535 multiple sclerosis; RRMS = relapsing-remitting multiple sclerosis.
536

(NEW) Table e-2 Specific genes/pathways in mice most impacted by DMF and MEF

Pathways	Gene Symbols	-log (P-value)
Interaction Pathways		
Aldosterone Signaling in Epithelial Cells	DNAJA1, DNAJB1, HSPA8, HSPH1, SOS1	3.13E+00
Assembly of RNA Polymerase III Complex	GTF3C4, GTF3C2	2.79E+00
Unfolded protein response	Hspa1b, HSPA8, HSPH1	2.68E+00
Huntington's Disease Signaling	Hspa1b, DNAJB1, HSPA8, NCOR1, SOS1	2.34E+00
DMF-specific Pathways		
NRF2-mediated Oxidative Stress Response	SQSTM1, GSTA3, GSTA5, GCLC, CBR1, TXN, NQO1, GSTK1, MGST1, PRDX1, GSTM1, GSTM5, CAT, AOX1, MAFG, FTL, GSTP1, FTH1	9.27E+00
Xenobiotic Metabolism Signaling	GSTA3, GSTA5, GCLC, UGT2B7, UGT1A9 (includes others), CAMK2D, Ces1g, NQO1, GSTK1, MGST1, ESD, GSTM1, GSTM5, CAT, UGT2B28, FTL, NDST1, GSTP1, ABCC3, UGT1A6	7.92E+00
Glutathione-mediated Detoxification	GSTA3, GSTA5, GSTM1, GSTM5, GSTP1, GSTK1, MGST1	6.48E+00
Aryl Hydrocarbon Receptor Signaling	GSTA3, GSTA5, GSTM1, GSTM5, RBL1, NQO1, GSTP1, GSTK1, CTSD, MGST1	4.13E+00
Nicotine Degradation III	UGT2B7, UGT1A9 (includes others), AOX1, UGT2B28, Aox3, UGT1A6	3.71E+00
Formaldehyde Oxidation II (Glutathione-dependent)	ADH5, ESD	3.61E+00
Nicotine Degradation II	UGT2B7, UGT1A9 (includes others), AOX1, UGT2B28, Aox3, UGT1A6	3.34E+00
Serotonin Degradation	UGT2B7, UGT1A9 (includes others), ADH5, ALDH2, UGT2B28, UGT1A6	3.30E+00
LPS/IL-1 Mediated Inhibition of RXR Function	GSTA3, GSTA5, GSTM1, GSTM5, CAT, APOE, NDST1, GSTP1, GSTK1, MGST1, ABCC3	3.14E+00
Thyroid Hormone Metabolism II (via Conjugation and/or Degradation)	UGT2B7, UGT1A9 (includes others), UGT2B28, UGT1A6	2.67E+00
Pentose Phosphate Pathway (Oxidative Branch)	PGD, G6PD	2.62E+00

Pathways	Gene Symbols	-log (P-value)
Glutathione Redox Reactions I	PRDX6, GSTK1, MGST1	2.51E+00
Superoxide Radicals Degradation	CAT, NQO1	2.31E+00
Estrogen-mediated S-phase Entry	E2F6, SKP2, RBL1	2.22E+00
Role of BRCA1 in DNA Damage Response	E2F6, RFC1, FAM175A, SMARCA2, RBL1	2.12E+00
MEF-specific Pathways		
RhoA Signaling	MYL12B, PIP5K1A, ROCK1, CDC42EP3, ACTR3, RDX	3.10E+00
Apoptosis Signaling	MAP2K7, KRAS, PARP1, ROCK1, CYCS	2.92E+00
Signaling by Rho Family GTPases	MAP2K7, GNG5, MYL12B, PIP5K1A, ROCK1, CDC42EP3, ACTR3, RDX	2.91E+00
Death Receptor Signaling	MAP2K7, PARP1, TNKS2, ROCK1, CYCS	2.86E+00
Sphingosine and Sphingosine-1-phosphate Metabolism	SGPP1, ASAH1	2.67E+00
fMLP Signaling in Neutrophils	KRAS, Calm1 (includes others), GNG5, PPP3CB, ACTR3	2.55E+00
Cardiac Hypertrophy Signaling	MAP2K7, KRAS, Calm1 (includes others), GNG5, MYL12B, PPP3CB, ROCK1	2.41E+00
autophagy	NBR1, LAMP2, BECN1	2.40E+00
RhoGDI Signaling	GNG5, MYL12B, PIP5K1A, ROCK1, ACTR3, RDX	2.34E+00
Ephrin Receptor Signaling	KRAS, GNG5, RAP1B, ABI1, ROCK1, ACTR3	2.32E+00
B Cell Receptor Signaling	MAP2K7, KRAS, BCL6, Calm1 (includes others), RAP1B, PPP3CB	2.30E+00
Role of NFAT in Cardiac Hypertrophy	MAP2K7, CSNK1A1, KRAS, Calm1 (includes others), GNG5, PPP3CB	2.27E+00
Regulation of IL-2 Expression in Activated and Anergic T Lymphocytes	MAP2K7, KRAS, Calm1 (includes others), PPP3CB	2.26E+00
Axonal Guidance Signaling	KRAS, GNG5, TUBB6, MYL12B, NRP1, RAP1B, PPP3CB, ROCK1, BRCC3, ACTR3	2.25E+00
Regulation of the Epithelial-Mesenchymal Transition Pathway	MAP2K7, ESRP2, KRAS, PSEN2, FRS2, ZEB2	2.21E+00
Telomere Extension by Telomerase	TNKS2, HNRNPA2B1	2.11E+00

Pathways	Gene Symbols	-log (P-value)
UVA-Induced MAPK Signaling	KRAS, PARP1, TNKS2, CYCS	2.10E+00
Granzyme B Signaling	PARP1, CYCS	2.06E+00
Regulation of Actin-based Motility by Rho	MYL12B, PIP5K1A, ROCK1, ACTR3	2.05E+00
RAN Signaling	RAN, KPNB1	2.01E+00

538 Abbreviations: DMF = dimethyl fumarate; MEF = monoethyl fumarate; MS = multiple sclerosis; RRMS = relapsing-

539 remitting multiple sclerosis.

540

541

542

543 **(NEW) Table e-3 Specific pathways in mice most impacted by a combination of DMF and MEF**

Tissue	Ingenuity Canonical Pathways	Proportion of pathway molecules represented in DEG list	Molecules	Pvalue
Blood	Aryl Hydrocarbon Receptor Signaling	1.17E-02	NQO1,TGM2	1.10E-03
Blood	Superoxide Radicals Degradation	1.25E-01	NQO1	2.19E-03
Blood	Pregnenolone Biosynthesis	7.69E-02	MICAL3	2.19E-03
Blood	Histidine Degradation VI	5.00E-02	MICAL3	3.31E-03
Blood	Ubiquinol-10 Biosynthesis (Eukaryotic)	3.33E-02	MICAL3	4.79E-03
Brain	Superoxide Radicals Degradation	1.25E-01	NQO1	6.31E-04
Brain	Nicotine Degradation III	1.37E-02	Aox3	5.37E-03
Brain	Nicotine Degradation II	1.18E-02	Aox3	6.31E-03
Brain	Hypoxia Signaling in the Cardiovascular System	1.47E-02	NQO1	6.92E-03
ILN	Aryl Hydrocarbon Receptor Signaling	1.17E-02	GSTM5,NQO1	7.76E-04
ILN	NRF2-mediated Oxidative Stress Response	1.03E-02	GSTM5,NQO1	1.29E-03
ILN	Superoxide Radicals Degradation	1.25E-01	NQO1	1.86E-03
ILN	Xenobiotic Metabolism Signaling	6.94E-03	GSTM5,NQO1	2.88E-03
ILN	Glutathione-mediated Detoxification	2.27E-02	GSTM5	8.71E-03
Jejunum	Xenobiotic Metabolism Signaling	5.56E-02	ABCC2,ABCC3,ALDH1A1,CES1,Ces1e ,GCLC,GSTA3,GSTA5,GSTK1,GSTM1,	1.58E-18

			Gstm3,GSTM4,GSTM5,NQO1,UGT2B15,UGT2B7	
Jejunum	Glutathione-mediated Detoxification	1.82E-01	GSTA3,Gsta4,GSTA5,GSTK1,GSTM1,Gstm3,GSTM4,GSTM5	2.00E-15
Jejunum	NRF2-mediated Oxidative Stress Response	5.64E-02	ABCC2,CBR1,GCLC,GSTA3,GSTA5,GSTK1,GSTM1,Gstm3,GSTM4,GSTM5,NQO1	5.01E-13
Jejunum	LPS/IL-1 Mediated Inhibition of RXR Function	4.49E-02	ABCC2,ABCC3,ACOX2,ALDH1A1,GSTA3,GSTA5,GSTK1,GSTM1,Gstm3,GSTM4,GSTM5	5.01E-12
Jejunum	Aryl Hydrocarbon Receptor Signaling	5.26E-02	ALDH1A1,GSTA3,GSTA5,GSTK1,GSTM1,Gstm3,GSTM4,GSTM5,NQO1	5.01E-11
Jejunum	PXR/RXR Activation	5.43E-02	ABCC2,ABCC3,ALDH1A1,Aldh1a7,GSTM1	6.17E-07
Jejunum	Serotonin Degradation	5.13E-02	ALDH1A1,Aldh1a7,UGT2B15,UGT2B7	1.51E-05
Jejunum	Glutathione Biosynthesis	1.82E-01	GCLC,GSS	1.78E-05
Jejunum	Histamine Degradation	6.90E-02	ALDH1A1,Aldh1a7	4.47E-04
Jejunum	Î³-glutamyl Cycle	7.14E-02	GCLC,GSS	6.03E-04
Jejunum	Fatty Acid Î±-oxidation	8.70E-02	ALDH1A1,Aldh1a7	6.92E-04
Jejunum	Oxidative Ethanol Degradation III	5.00E-02	ALDH1A1,Aldh1a7	6.92E-04
Jejunum	Putrescine Degradation III	6.67E-02	ALDH1A1,Aldh1a7	7.76E-04
Jejunum	Tryptophan Degradation X (Mammalian, via Tryptamine)	6.90E-02	ALDH1A1,Aldh1a7	8.71E-04
Jejunum	Ethanol Degradation IV	6.90E-02	ALDH1A1,Aldh1a7	8.71E-04
Jejunum	Dopamine Degradation	5.26E-02	ALDH1A1,Aldh1a7	1.58E-03

Jejunum	Sorbitol Degradation I	2.00E-01	SORD	2.45E-03
Jejunum	Retinoate Biosynthesis I	5.41E-02	AKR1B10,ALDH1A1	2.82E-03
Jejunum	Thyroid Hormone Metabolism II (via Conjugation and/or Degradation)	3.77E-02	UGT2B15,UGT2B7	2.82E-03
Jejunum	Ethanol Degradation II	4.65E-02	ALDH1A1,Aldh1a7	2.95E-03
Jejunum	Retinol Biosynthesis	4.44E-02	CES1,Ces1e	3.31E-03
Jejunum	Noradrenaline and Adrenaline Degradation	3.77E-02	ALDH1A1,Aldh1a7	3.55E-03
Jejunum	Nicotine Degradation III	2.74E-02	UGT2B15,UGT2B7	7.24E-03
Jejunum	L-serine Degradation	1.67E-01	SRR	7.41E-03
Jejunum	Melatonin Degradation I	3.03E-02	UGT2B15,UGT2B7	8.13E-03
Jejunum	Superpathway of Melatonin Degradation	2.47E-02	UGT2B15,UGT2B7	9.55E-03
Jejunum	Heme Degradation	9.09E-02	BLVRB	9.77E-03
Jejunum	Nicotine Degradation II	2.35E-02	UGT2B15,UGT2B7	9.77E-03
Kidney	LXR/RXR Activation	6.47E-02	ALB,APOA1,APOC1,APOC2,APOC3,APOE,GC,SERPINA1,TTR	7.41E-08
Kidney	LPS/IL-1 Mediated Inhibition of RXR Function	4.49E-02	ALAS1,ALDH3A1,APOC1,APOC2,APOE,FABP5,GSTA3,Gstm3,GSTM4,GSTM5,GSTP1	1.58E-07
Kidney	NRF2-mediated Oxidative Stress Response	5.13E-02	AOX1,EPHX1,GSR,GSTA3,Gstm3,GSTM4,GSTM5,GSTP1,HMOX1,NQO1	2.14E-07
Kidney	Glutathione-mediated Detoxification	1.14E-01	GSTA3,Gstm3,GSTM4,GSTM5,GSTP1	8.13E-07
Kidney	Atherosclerosis Signaling	5.76E-02	ALB,APOA1,APOC1,APOC2,APOC3,APOE,PLA2G7,SERPINA1	1.07E-06

Kidney	Xenobiotic Metabolism Signaling	3.82E-02	ALDH3A1,Ces2b/Ces2c,GSTA3,Gstm3,GSTM4,GSTM5,GSTP1,HMOX1,NQO1,UGT2B10,UGT2B15	1.20E-06
Kidney	Nicotine Degradation III	6.85E-02	AOX1,CYP2D6,CYP2J2,UGT2B10,UGT2B15	1.91E-05
Kidney	IL-12 Signaling and Production in Macrophages	4.46E-02	ALB,APOA1,APOC1,APOC2,APOC3,APOE,SERPINA1	2.29E-05
Kidney	Clathrin-mediated Endocytosis Signaling	4.04E-02	ALB,APOA1,APOC1,APOC2,APOC3,APOE,ITGB6,SERPINA1	2.29E-05
Kidney	Aryl Hydrocarbon Receptor Signaling	4.09E-02	ALDH3A1,GSTA3,Gstm3,GSTM4,GSTM5,GSTP1,NQO1	3.02E-05
Kidney	Pentose Phosphate Pathway	1.30E-01	G6PD,PGD,TKT	3.89E-05
Kidney	Nicotine Degradation II	5.88E-02	AOX1,CYP2D6,CYP2J2,UGT2B10,UGT2B15	4.17E-05
Kidney	Production of Nitric Oxide and Reactive Oxygen Species in Macrophages	3.30E-02	ALB,APOA1,APOC1,APOC2,APOC3,APOE,SERPINA1	1.41E-04
Kidney	Heme Degradation	1.82E-01	BLVRB,HMOX1	2.34E-04
Kidney	Pentose Phosphate Pathway (Oxidative Branch)	1.82E-01	G6PD,PGD	3.89E-04
Kidney	Melatonin Degradation I	6.06E-02	CYP2D6,CYP2J2,UGT2B10,UGT2B15	3.98E-04
Kidney	Superpathway of Melatonin Degradation	4.94E-02	CYP2D6,CYP2J2,UGT2B10,UGT2B15	5.62E-04
Kidney	Coagulation System	7.89E-02	PLAU,PLAUR,SERPINA1	1.38E-03
Kidney	FXR/RXR Activation	3.64E-02	APOA1,APOC2,APOC3,APOE	2.14E-03
Kidney	Acute Phase Response Signaling	2.76E-02	ALB,APOA1,HMOX1,SERPINA1,TTR	4.37E-03
Kidney	Serotonin Degradation	3.85E-02	ALDH3A1,UGT2B10,UGT2B15	6.76E-03

MLN	Airway Pathology in Chronic Obstructive Pulmonary Disease	1.82E-01	MMP2,MMP9	1.00E-04
MLN	NRF2-mediated Oxidative Stress Response	2.05E-02	GSTA3,GSTM5,HMOX1,NQO1	3.89E-04
MLN	Glutathione-mediated Detoxification	4.55E-02	GSTA3,GSTM5	1.32E-03
MLN	Xenobiotic Metabolism Signaling	1.39E-02	GSTA3,GSTM5,HMOX1,NQO1	1.78E-03
MLN	Hepatic Fibrosis / Hepatic Stellate Cell Activation	1.94E-02	AGTR1,MMP2,MMP9	2.40E-03
MLN	Aryl Hydrocarbon Receptor Signaling	1.75E-02	GSTA3,GSTM5,NQO1	2.45E-03
MLN	Inhibition of Matrix Metalloproteases	5.00E-02	MMP2,MMP9	2.57E-03
MLN	IL-8 Signaling	1.33E-02	HMOX1,MMP2,MMP9	5.62E-03
MLN	Glioma Invasiveness Signaling	3.03E-02	MMP2,MMP9	5.62E-03
MLN	Eicosanoid Signaling	2.33E-02	LTC4S,PTGDS	6.61E-03
MLN	Heme Degradation	9.09E-02	HMOX1	7.76E-03
MLN	LPS/IL-1 Mediated Inhibition of RXR Function	1.22E-02	GSTA3,GSTM5,HMGCS2	8.71E-03
Spleen	NRF2-mediated Oxidative Stress Response	1.54E-02	AOX1,GSTA3,GSTM5	8.13E-06
Spleen	Glutathione-mediated Detoxification	4.55E-02	GSTA3,GSTM5	2.04E-05
Spleen	Aryl Hydrocarbon Receptor Signaling	1.17E-02	GSTA3,GSTM5	5.25E-04
Spleen	LPS/IL-1 Mediated Inhibition of RXR Function	8.16E-03	GSTA3,GSTM5	1.29E-03
Spleen	Xenobiotic Metabolism Signaling	6.94E-03	GSTA3,GSTM5	1.95E-03
Spleen	Guanosine Nucleotides Degradation III	4.35E-02	AOX1	3.39E-03

Spleen	Urate Biosynthesis/Inosine 5'-phosphate Degradation	4.35E-02	AOX1	3.63E-03
Spleen	Adenosine Nucleotides Degradation II	3.57E-02	AOX1	4.47E-03
Spleen	Purine Nucleotides Degradation II (Aerobic)	2.70E-02	AOX1	5.25E-03

544 Abbreviations: DEG = differentially expressed gene; ILN = inguinal lymph node; MLN = mesenteric lymph node.

545 Pathways with significant changes ($p<0.01$) after treatment of mice with the combination of DMF and MEF.

546 Pathways with significant changes ($p<0.01$) after treatment of mice with the combination of DMF and MEF.

Figure e-1 Steady-state tissue-specific DEGs in response to chronic DMF, MEF, and DMF/MEF administration in mice

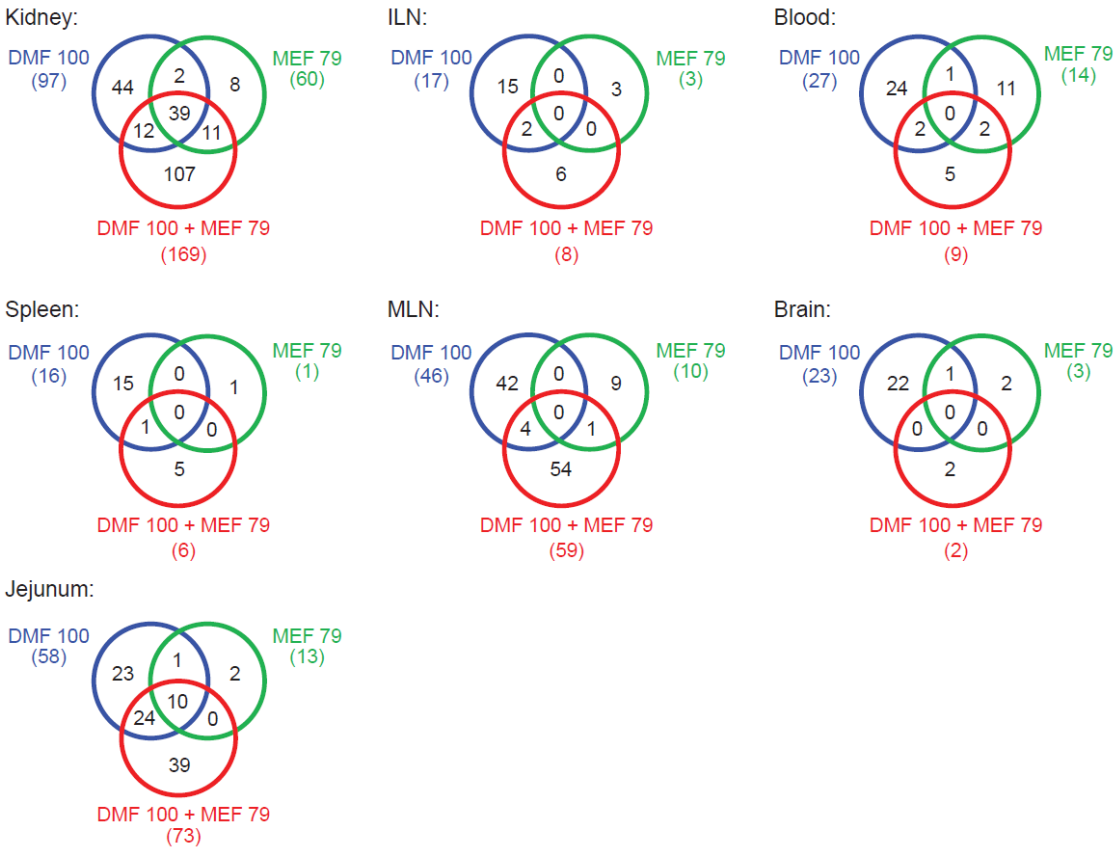

Tissue was harvested after 10 days of daily treatment with DMF, MEF, or DMF/MEF. DEGs were identified by comparing the groups DMF-vs-vehicle, MEF-vs-vehicle, and DMF/MEF-vs-vehicle in each tissue. The number in parentheses designates the total number of DEGs for that treatment. DEG = differentially expressed gene; DMF = dimethyl fumarate; ILN = inguinal lymph node; MLN = mesenteric lymph node; MEF = monoethyl fumarate.

558 **Appendix 1** Author Contributions

Name	Location	Contribution
Brian T. Wipke, PhD	Biogen, Inc., Cambridge, MA	Designed and conceptualized study, interpreted the data, drafted the manuscript for intellectual content, revised the manuscript for intellectual content
Robert Hoepner, MD PhD	Inselspital, Bern University Hospital, University of Bern, Switzerland	Generated, analyzed, and interpreted data; revised manuscript for intellectual content
Katrin Strassburger-Krogias, MD	St. Josef Hospital, Ruhr University Bochum, Germany	Role in acquisition of data, interpreted the data, revised the manuscript for intellectual content
Ankur Thomas, MS	Biogen, Inc., Cambridge, MA	Designed and conceptualized study; major role in acquisition of data; generated, analyzed and interpreted data; revised manuscript for intellectual content
Davide Gianni, PhD	Biogen, Inc., Cambridge, MA	Designed and conceptualized study; major role in acquisition of data; generated, analyzed and interpreted data; revised manuscript for intellectual content
Suzanne Szak, PhD	Biogen, Inc., Cambridge, MA	Analyzed the data; interpreted the data; major role in revising the manuscript for intellectual content
Melanie S. Brennan, PhD	Biogen, Inc., Cambridge, MA	Generated, analyzed and interpreted data, revised manuscript for intellectual content
Maximilian Pistor, MD	Inselspital, Bern University Hospital, University of Bern, Switzerland	Analyzed the data; interpreted the data
Ralf Gold, MD, PhD	St. Josef Hospital, Ruhr University Bochum, Germany	Major role in study design and drafting of the manuscript; revised manuscript for intellectual content
Andrew Chan, MD	Inselspital, Bern University Hospital, University of Bern, Switzerland	Designed and conceptualized study; drafted the manuscript for intellectual content; major role in the acquisition of data; interpreted the data; revised the manuscript for intellectual content
Robert H. Scannevin, PhD	Biogen, Inc., Cambridge, MA	Design and conceptualized study, analyzed the data, drafted the manuscript for intellectual content, major role in the acquisition of data, interpreted the data, revised the manuscript for intellectual content

559

References (max 40)

1. Thompson AJ, Baranzini SE, Geurts J, Hemmer B, Ciccarelli O. Multiple sclerosis. Lancet 2018;391:1622-1636.

2. Mahad D, Ziabreva I, Lassmann H, Turnbull D. Mitochondrial defects in acute multiple sclerosis lesions. Brain 2008;131:1722-1735.

3. Biogen Inc. TECFIDERA® (dimethyl fumarate) delayed-release capsules, for oral use [online]. Available at: https://www.tecfidera.com/content/dam/commercial/multiple-sclerosis/tecfidera/pat/en_us/pdf/full-prescribing-info.pdf. Accessed July 26, 2019.

4. European Medicines Agency. Tecfidera 120 mg gastro-resistant hard capsules. Summary of product characteristics [online]. Available at: https://www.ema.europa.eu/documents/product-information/tecfidera-epar-product-information_en.pdf. Accessed July 26, 2019.

5. Schimrigk S, Brune N, Hellwig K, et al. Oral fumaric acid esters for the treatment of active multiple sclerosis: an open-label, baseline-controlled pilot study. Eur J Neurol 2006;13:604-610.

6. Scannevin RH, Chollate S, Jung MY, et al. Fumarates promote cytoprotection of central nervous system cells against oxidative stress via the nuclear factor (erythroid-derived 2)-like 2 pathway. J Pharmacol Exp Ther 2012;341:274-284.

7. Brennan MS, Matos MF, Li B, et al. Dimethyl fumarate and monoethyl fumarate exhibit differential effects on KEAP1, NRF2 activation, and glutathione depletion in vitro. PLoS One 2015;10:e0120254.

584 8. Gillard GO, Collette B, Anderson J, et al. DMF, but not other fumarates,
585 inhibits NF-κB activity in vitro in an Nrf2-independent manner. J Neuroimmunol
586 2015;283:74-85.
587 9. Höxtermann S, Nüchel C, Altmeyer P. Fumaric acid esters suppress
588 peripheral CD4- and CD8-positive lymphocytes in psoriasis. Dermatology
589 1998;196:223-230.
590 10. Fox RJ, Chan A, Gold R, et al. Characterizing absolute lymphocyte count
591 profiles in dimethyl fumarate-treated patients with MS: patient management
592 considerations. Neurol Clin Pract 2016;6:220-229.
593 11. Banerjee D, Zhao L, Wu L, et al. Small molecule mediated inhibition of
594 RORγ-dependent gene expression and autoimmune disease pathology in vivo.
595 Immunology 2016;147:399-413.
596 12. Ranger A, Ray S, Szak S, et al. Anti-LINGO-1 has no detectable
597 immunomodulatory effects in preclinical and phase 1 studies. Neurol
598 Neuroimmunol Neuroinflamm 2018;5:e417.
599 13. Irizarry RA, Bolstad BM, Collin F, Cope LM, Hobbs B, Speed TP.
600 Summaries of Affymetrix GeneChip probe level data. Nucleic Acids Res
601 2003;31:e15.
602 14. Li C, Hung Wong W. Model-based analysis of oligonucleotide arrays:
603 model validation, design issues and standard error application. Genome Biol
604 2001;2:research0032.0031.

15. Smyth GK. Linear models and empirical Bayes methods for assessing differential expression in microarray experiments. Stat Appl Genet Mol Biol 2004;3:Article3.

16. Bioinformatics and Computational Biology Solutions Using R and Bioconductor, 1st ed. New York: Springer-Verlag, 2005.

17. Strassburger-Krogias K, Ellrichmann G, Krogias C, Altmeyer P, Chan A, Gold R. Fumarate treatment in progressive forms of multiple sclerosis: first results of a single-center observational study. Ther Adv Neurol Disord 2014;7:232-238.

18. Ghoreschi K, Brück J, Kellerer C, et al. Fumarates improve psoriasis and multiple sclerosis by inducing type II dendritic cells. J Exp Med 2011;208:2291-2303.

19. Kornberg MD, Bhargava P, Kim PM, et al. Dimethyl fumarate targets GAPDH and aerobic glycolysis to modulate immunity. Science 2018;360:449-453.

20. Lehmann JC, Listopad JJ, Rentzsch CU, et al. Dimethylfumarate induces immunosuppression via glutathione depletion and subsequent induction of heme oxygenase 1. J Invest Dermatol 2007;127:835-845.

21. Tang H, Lu JY, Zheng X, Yang Y, Reagan JD. The psoriasis drug monomethylfumarate is a potent nicotinic acid receptor agonist. Biochem Biophys Res Commun 2008;375:562-565.

626 22. Schulze-Topphoff U, Varrin-Doyer M, Pekarek K, et al. Dimethyl fumarate
627 treatment induces adaptive and innate immune modulation independent of Nrf2.
628 Proc Natl Acad Sci U S A 2016;113:4777-4782.
629 23. Scannevin RH, Chollate S, Jung MY, et al. Fumarates promote
630 cytoprotection of central nervous system cells against oxidative stress via the
631 nuclear factor (erythroid-derived 2)-like 2 pathway. J Pharmacol Exp Ther
632 2012;341:274-284.
633 24. Bhargava P, Fitzgerald KC, Venkata SLV, et al. Dimethyl fumarate
634 treatment induces lipid metabolism alterations that are linked to immunological
635 changes. Ann Clin Transl Neurol 2019;6:33-45.
636 25. Spencer CM, Crabtree-Hartman EC, Lehmann-Horn K, Cree BAC, Zamvil
637 SS. Reduction of CD8(+) T lymphocytes in multiple sclerosis patients treated with
638 dimethyl fumarate. Neurol Neuroimmunol Neuroinflamm 2015;2:e76.
639 26. Mehta D, Miller C, Arnold DL, et al. Effect of dimethyl fumarate on
640 lymphocytes in RRMS: implications for clinical practice. Neurology
641 2019;92:e1724-e1738.
642 27. Robb J, Hyland M, Samkoff L. Dimethyl fumarate-associated lymphopenia
643 in clinical practice: implications for disease modifying therapy selection.
644 Neurology 2016;86:P6.192.
645 28. Gold R, Kappos L, Arnold DL, et al. Placebo-controlled phase 3 study of
646 oral BG-12 for relapsing multiple sclerosis. N Engl J Med 2012;367:1098-1107.

29. Fox RJ, Miller DH, Phillips JT, et al. Placebo-controlled phase 3 study of oral BG-12 or glatiramer in multiple sclerosis. N Engl J Med 2012;367:1087-1097.

30. Fox RJ, Chan A, Gold R. Characterization of absolute lymphocyte count profiles in MS patients treated with delayed-release dimethyl fumarate: considerations for patient management. Mult Scler J 2015;21:P606.